CUDC-101 is a potential target inhibitor for the EGFR-overexpression bladder cancer cells

ZHENXING WANG[1*], LANXIN LI[1*], CHUNHONG CHU[2,3*], XIANGKAI WEI[4], QIAN LIU[4], RUI WANG[1], GUOLIANG ZHANG[2,3], GUANGYAO WU[1], YING WANG[4], LEI AN[1,3] and XIAODONG LI[1]

[1]Translational Medicine Center, Huaihe Hospital of Henan University, [2]School of Pharmacy, [3]Institutes of Traditional Chinese Medicine and [4]Department of Anesthesiology, The First Affiliated Hospital of Henan University, Henan University, Kaifeng, Henan 475000, P.R. China

Received May 19, 2023; Accepted September 19, 2023

DOI: 10.3892/ijo.2023.5579

Abstract. Bladder cancer is one of the most common urological malignancies worldwide. The molecular mechanism underlying its development is complex, but its carcinogenesis has been proposed to occur with cell proliferation and resistance to apoptosis, driven by the signaling activity of abundant EGFR and receptor tyrosine-protein kinase erbB-2. In the present study, T24 bladder cancer cell lines with EGFR-overexpression were constructed, before the multi-target inhibitor CUDC-101 was used to investigate its potential as a targeted therapeutic agent for bladder cancer using chemosensitivity methods. The results showed that CUDC-101 induced cytotoxic effects, inhibited growth vitality and proliferation in a dose-dependent manner. CUDC-101 also altered the skeletal morphology and microfilament structure, while blocking cell cycle progression and causing apoptosis. These results supported the proposed cytotoxic effects of CUDC-101, in addition to its inhibitory effects on cell division and proliferation in EGFR-overexpressing bladder cancer cells. Therefore CUDC-101 may to be a potential therapeutic option for the treatment of bladder cancer.

Introduction

Bladder cancer is one of the most common cancers in the world population and the most common urological malignancy (1). Its pathogenesis is complex with the risk varying by sex, intrinsic genetic factors and age. In addition, it is heavily influenced by the degree of exposure to a number of carcinogens due to different life circumstances, such as smoking (2). Treatment of early bladder cancer is primarily by surgical resection, but surgical intervention is general ineffective for patients with advanced disease or developed metastases (3). Further understanding of bladder cancer through molecular biology and genetics studies has led to the development of diagnostic and therapeutic modalities for localized and advanced bladder cancer. Notable breakthroughs include intravesical infusion of bacilli Calmette-Guerin vaccine, immunotherapy with checkpoint inhibition, targeted therapy and antibody-drug adjuvants (4). However, bladder cancer is a molecularly heterogeneous disease, where genomic expression analysis has shown that different expression profiles are associated with different profiles of cancer progression and metastasis (5). Based on the different gene expression profiles, selection of the optimal therapeutic approach has become a key factor for increasing the efficacy of bladder cancer treatment.

In a variety of solid tumors, such as breast (6), lung (7), colon (8), ovarian, bladder, prostate, head and neck tumors (9,10). EGFR has been reported to serve an important role in cell origin, apoptosis, tumor vascularization and metastasis (11,12). In particular, receptor tyrosine-protein kinase erbB HER-1 and HER-2, being similar in structure and function, serves key roles in tumorigenesis and share homologous sequences with expressed oncogenes and/or viral oncogenes (13).

CUDC-101, a multipathway inhibitor, has been reported to inhibit both histone deacetylases (HDAC) and receptor kinases (14). Additionally, CUDC-101 combined with HDAC inhibition was found to block the key regulator of the EGFR/HER2 signaling pathway synergistically and attenuated multiple surrogate pathways. This enhanced the potential for treating heterogeneous and resistant tumors that cannot be controlled by single-target drugs (15,16). It also showed a favorable preclinical safety profile in a Phase I clinical trial and had no effect on the growth of normal urinary tract epithelial cells (17) and CUDC-101 was developed as a novel anti-cancer drug (18).

At present, targeted therapies for bladder cancer in the presence of EGFR are poorly studied. In order to explore targeted agents for the treatment of bladder cancer, the present study chose this multipathway inhibitor to test its effect on the growth of EGFR overexpressing bladder cancer cells.

Correspondence to: Professor Lei An or Professor Xiaodong Li, Translational Medicine Center, Huaihe Hospital of Henan University, Henan University, 115 Ximen Avenue, Kaifeng, Henan 475000, P.R. China
E-mail: anlei@henu.edu.cn
E-mail: hhyylxd2013@126.com

*Contributed equally

Key words: bladder cancer, CUDC-101, EGFR, proliferation, cytotoxicology

Materials and methods

Drugs and reagents. Human bladder cancer T24 cell was purchased from Procell Life Science & Technology Co., Ltd. Human embryonic kidney cell 293T was purchased from Gaining Biological. CUDC-101 was purchased from Selleck Chemicals. All molecular cloning reagents were purchased from New England Biolabs, Inc. MTT, protease inhibitor cocktail, Halt phosphatase inhibitor cocktail, BCA protein quantification kit were purchased from Beijing Solarbio Science & Technology Co., Ltd. BeyoClick EdU cell proliferation kit with Alexa Fluor 555 (cat. no. C0075S), mitochondrial membrane potential and apoptosis detection kit with Mito-Tracker Red CMXRos (cat. no. C1071M), Annexin V-FITC, FITC annexin V solution and PI (cat. no. ST512) were purchased from Beyotime Institute of Biotechnology. All antibodies were purchased from Proteintech Group, Inc. Blasticidin (BSD) was purchased from Thermo Fisher Scientific, Inc. RPMI1640 complete medium, DMEM, FBS, penicillin and streptomycin were purchased from Gibco (Thermo Fisher Scientific, Inc.). The fluorescent microscope used was Eclipse Ti (Nikon Corporation). The flow cytometer used was BD FACSCanto (BD Biosciences).

Cell culture. The medium used for 293T cells was DMEM containing 10% FBS, 100 U/ml penicillin and 100 μg/ml streptomycin. The medium used for the human bladder cancer cell lines T24 (bladder cell lines) was RPMI1640 complete medium containing 10% FBS, 100 U/ml penicillin and 100 μg/ml streptomycin. The medium used for T24-EGFR-everexpressing (EGFR-OE) cells was RPMI1640 complete medium containing 10% FBS, 100 U/ml penicillin, 100 μg/ml streptomycin and 10 μg/ml BSD-HCl. All cells were cultured in a cell culture incubator at 37˚C, and 5% CO_2 with saturated humidity. Cells were passaged at logarithmic growth phases and frozen for storage according to the experimental requirement.

Establishment of the T24-EGFR-OE cell line. The 293T cells were cultured in six-well plates and co-transfected with the pLenti-EF1α plasmid containing the wild-type EGFR gene (deposited in the Laboratory of the Translational Center of Huaihe Hospital, Henan University) and two packaging plasmids psPAX2 and pMD2.G (deposited in the Laboratory of the Translational Center of Huaihe Hospital, Henan University) at a 1:1:1 molar ratio using the cationic polymer transfection reagent (EZ Trans cell transfection reagent; Life-iLab) when cell confluency reached 80%. Cells were grown for 16 h at 37˚C in a humidified atmosphere with 5% CO_2 before being replaced with fresh medium. After a further 48 h, the cell supernatant containing the viral particles were collected and filtered through a 0.45-μM filter before being added to T24 cells when they reached 80% confluency. At 24 h later, the culture medium of T24 cells was replaced with a fresh medium. After another 48 h, a medium containing 10 μg/ml BSD was added for 14 days for screening.

Cell survival and viability assays. MTT assay was used for cell survival and viability assays. T24 and T24-EGFR-OE cells in the logarithmic growth phase were seeded into 96-well plates at a density of 5,000 cells per well. After 18 h, the medium from each well was removed, before 100 μl of medium containing different concentrations of CUDC-101 was added and incubated for 48 h. Subsequently, 20 μl of MTT was added, before incubation continued for a further 4 h in an incubator at 37˚C. The supernatant was then discarded at the end of the culture and 100 μl DMSO solution was added into each well. The plates were placed in a shaker at 37˚C under light-proof conditions for 15 min, before the optical density (OD) was measured using a microplate reader.

Transcriptome sequencing. Cells in the logarithmic growth phase were seeded into 10-cm dishes at a density of ~5 million cells per well, where they were left to stably attached to the bottom of the dish. The medium was then aspirated before 1 μM of the CUDC-101 was added. The reaction was terminated after 48 h of drug treatment, before total cellular RNA was extracted by TRIzol® lysis, chloroform separation, and RNA precipitation with isoamyl alcohol and anhydrous ethanol. In total, three independent replicates were made for each sample and the extracted RNA was stored on dry ice.

Integrity of the test sample was detected by nucleic acid gel electrophoresis using a NanoDrop 2000 (Thermo Fisher Scientific, Inc.). The concentrations of each sample in the present study was >50 ng/μl and library concentration was ~7 pM with a volume of 30 μl for sequencing. The length bit was 150 bp and the sequencing direction was 'paired end'. The transcriptome data was performed using the Illumina sequencing platform [VAHTS Universal V8 RNA-seq Library Prep Kit for Illumina (Vazyme Biotech Co., Ltd.)] and the raw data were optimized to obtain high-quality clean reads. Differential gene analysis among the samples was performed using DESeq2 (all software provided by GoldViz Biotechnology Co., Ltd. https://www.genewiz.com.cn/). Fold Change (FC) was used to represents the ratio of expression between two sample groups, where the screening criteria were $Log_2FC > 2$ and $P \leq 0.05$. Multiple testing for statistically significant differences were corrected according to the false discovery rate. The differentially expressed genes were enriched in Gene Ontology (GO) and Kyoto Encyclopedia of Genes and Genomes (KEGG) databases (all software provided by GoldViz Biotechnology Co., Ltd., https://www.genewiz.com.cn/) to analyze the biochemical metabolic pathways and signal transduction pathways with which they are associated.

Cell proliferation assay. EdU was used for cell proliferation assay. Cells in the logarithmic growth phase were seed into 96-well plates at a density of 5,000 cells per well, before the medium in the wells was changed to CUDC-101-containing medium after 18 h before further culturing for 48 h at 37˚C. A total of 100 μl of EdU was added into each well, then cultured at 37˚C for 1 h. Afterwards, the medium was removed and the cells were fixed with 4% paraformaldehyde at 37˚C for 15 min, blocked with 3% bovine serum albumin in PBS at room temperature for 5 min and permeabilized in 0.3% Triton X-100 in PBS at room temperature for 5 min. The cells were then washed sequentially and 50 μl prepared click reaction solution was added to label proliferating cells in the dark at room temperature for 30 min. The medium was then removed and the cells were washed again, before 50 μl Hoechst was added to label all nuclei and incubated in the dark at room temperature

for 10 min. The cells were then immediately observed by fluorescence microscopy (CX31; Olympus Corporation).

Cell cycle assay. Cells in the logarithmic growth phase were seeded into six-well plates at a density of $6x10^5$ cells per well. After the cells completely adhered to the bottom of the dish, a medium containing different concentrations of CUDC-101 was added before culturing continued for 48 h at 37˚C. The medium was then removed and the cells were washed with PBS, before they were digested with 0.25% trypsin. These digested cells were collected and centrifuged at 600 x g for 5 min to remove the supernatant, before the tubes were transferred onto ice and the cells were slowly resuspended with pre-chilled 70% ethanol and left at -20˚C for 24 h. Cells were removed the next day and centrifuged at 1,000 x g for 5 min at 4˚C. The ethanol was removed and cells were resuspended in 1 ml ice-cold PBS, before they cells were centrifuged at 500 x g for 10 min at 4˚C and the PBS was removed. Cells were then resuspended in 0.5 ml of staining solution and incubated at 37˚C for 30 min in the dark. The cells were washed twice with PBS and resuspend with pre-chilled PBS. Cells were analyzed within 24 h by flow cytometry [CytoFLEX S; Bellman Coulter, Inc.; FlowJo v10.6.2 (FlowJo LLC) was used to analyze the data].

Colony formation assay. Cells in the logarithmic growth phase were seeded into six-well plates at a density of 500 cells per well and left to fully attach to the bottom. A medium containing different concentrations of CUDC-101 was added. The cells were incubated at 37˚C for 2 weeks, during which the medium was changed once every 3 days. When the colonies became visible in the dishes to with the naked eye, the culture was terminated and the medium was removed. The cells were fixed with 4% paraformaldehyde for 10 min and washed twice with PBS, before 1X Giemsa stain was added for 10 min at room temperature. Finally, PBS was rinsed and dried for imaging using a gel imager (ChemiDoc; Bio-Rad Laboratories, Inc.).

Cell morphology observation. Cells in the logarithmic growth phase were seeded into 12-well plates with cell crawling sheets at a density of $5x10^4$ per well. After the cells attached to the bottom, different concentrations of CUDC-101 were added to continue the culturing for 48 h. Subsequently, the cell supernatant was removed, the cells were washed with PBS for 5 min and fixed with paraformaldehyde for 10 min, before being treated with TRITC-phalloidin solution and DAPI solution for 10 min at room temperature. The cells were placed on cover slides in the bottom of the petri dish, before being imaged and observed by fluorescence microscopy after the adsorption was stabilized.

Mitochondrial membrane potential and apoptosis assay. Cells were seed into 96-well plates at a density of 5,000 per well and incubated at 37˚C for 18 h. The supernatant was then removed, before culture medium containing different concentrations of CUDC-101 was added and incubation continued for 48 h. The 96-well plates were removed and the cells were centrifuged at 1,000 x g for 5 min at room temperature, before the culture medium was removed. In total, 100 μl PBS was added to each well for washing, followed by centrifugation at 1,000 x g for 5 min at room temperature before removing the PBS. After removing PBS, 32 μl Annexin V-FITC conjugate was added into each well, before add 0.84 μl Annexin V-FITC staining solution, 0.34 μl Mito-Tracker Red CMXRos staining solution and 0.84 μl Hoechst 33342 staining solution were mixed gently and added into each well for incubation at room temperature in the dark for 20 min. Images were captured under a fluorescent microscope.

Flow cytometry for apoptosis. Cells in the logarithmic growth phase were seeded into six-well plates at a density of $6x10^5$ cells per well, before they were allowed adhered to the bottom completely. A medium containing different concentrations of CUDC-101 was then added culture at 37˚C for 48 h. Subsequently, the supernatant was aspirated into Eppendorf tubes, before the cells were washed with PBS and digested with 0.25% trypsin. The digested cells were then collected, mixed with supernatant and centrifuged in 1,000 x g for 5 min at room temperature, washed and resuspended again with PBS, stained with Annexin V-FITC and PI at room temperature for 15 min to label the apoptotic cells. Finally, the percentage of apoptosis was detected. Calculation of apoptosis rate was by the percentage of early + late apoptotic cells. Flow cytometer CytoFLEX S was used for the detection (Bellman Coulter, Inc.) and FlowJo v10.6.2 (FlowJo LLC) was used to analyze the data.

Western blot analysis. Cells in the logarithmic growth phase were seeded into six-well plates at a density of $6x10^5$ cells per well and were allowed to adhere to the bottom completely. Media containing different CUDC-101 concentrations was added for incubation for 48 h and the control group was only treated with 1640 medium. The cells were then lysed with RIPA lysis buffer (Shanghai Biyuntian Biotechnology Research Institute) to extract total cellular proteins. Protein determination was by BCA from Beijing Kangwei Century Co., Ltd. A total of 50 μg of protein was loaded per lane and separated on 10% gel before transfer to NC membrane. Blocking was by 5X loading buffer from Shanghai Biyuntian Biotechnology Co., Ltd at 100˚C for 5 min The following antibodies were used: Anti-Bcl-XL (1:2,000), anti-Bad (1:2,000), anti-heme oxygenase-1 (HO-1; 1:2,000), anti-ERK (1:2,000), anti-phosphorylated (p-) ERK (1:2,000), anti-AKT (1:1,000), anti-p-AKT (1:2,000), anti-EGFR (1:1,000), anti-p-EGFR (Cell Signaling Technology, 1:1,000, USA), anti-GAPDH (1:50,000), Goat Anti-Rabbit IgG (1:5,000), Goat Anti-Mouse IgG (1:5,000). All antibodies were purchased from Wuhan Sanying Biotechnology Co., Ltd. Primary antibody incubation was at 4˚C for 12 h and secondary antibody incubation was at room temperature for 1 h. ECL chemiluminescence kit purchased from Shanghai Biyuntian Biotechnology Co., Ltd. and ImageJ (version 1.53f51; National Institutes of Health) was used for densitometry.

Statistical analysis. All data are presented as the mean ± SEM. One-way ANOVA (with Bonferroni for post hoc test) was used for statistical comparisons between the groups. Tests were performed out using SPSS 21.0 software (IBM Corp.) and drawn using GraphPad Prism 8.0 software (GraphPad Software, Inc.; Dotmatics). Cutadapt (V1.9.1), Hisat2 (v2.0.1),

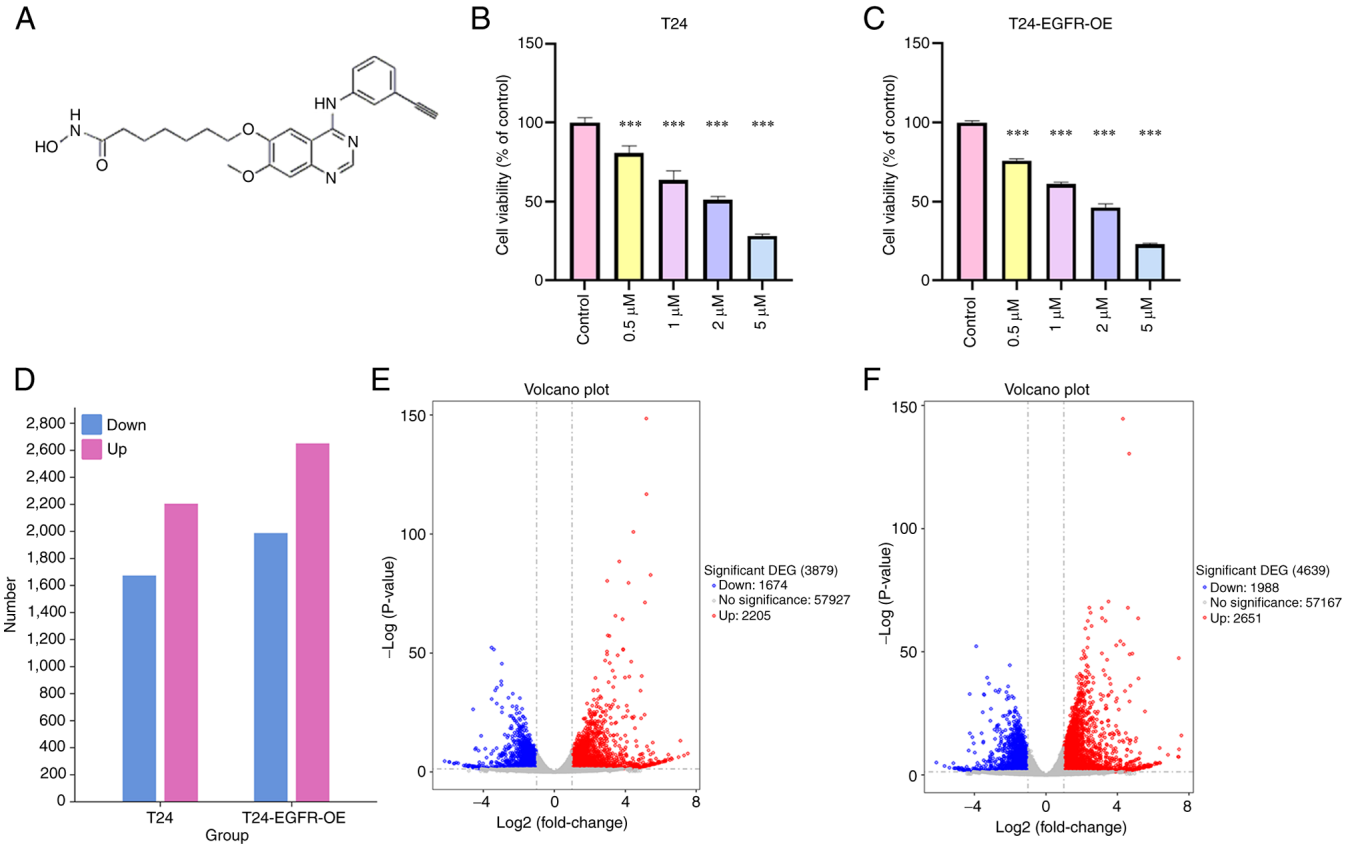

Figure 1. Effect of CUDC-101 on cell viability and gene expression. (A) The chemical formula of CUDC-101. The survival rates of (B) T24 cells and (C) T24-EGFR-OE cells after treatment with CUDC-101 at 0, 0.5, 1, 2 and 5 μM. The cell survival rate of the control group was set at 100%. Data are presented as mean ± SEM from three independent experiments. ***P<0.001 vs. control. (D) Histogram of the number of gene changes before and after drug treatment. The number of genes up- and downregulated after drug treatment in T24 (E) and T24-EGFR-OE cells (F). OE, overexpression; DEG, differentially expressed genes.

HTSeq (v0.6.1), were used for data processing and gene analysis. GOSeq (v1.34.1) was used for GO and KEGG analysis; all software provided by GoldViz Biotechnology Co., Ltd. (https://www.genewiz.com.cn/). Pearson correlation analysis was used to analyze RNA sample correlation on transcriptome sequencing. Raw data generated by Illumina transcriptome sequencing has been submitted to the NCBI public database (BioProject ID: PRJNA1010990).

Results

CUDC-101 decreases T24 cell viability. To investigate the effect of CUDC-101 on cell viability, T24 and T24-EGFR-OE cells were treated with different concentrations of CUDC-101 before being assayed using MTT method after 48 h. The results are shown in Fig. 1B and C. The cell viability of both cell types were decreased by CUDC-101 treatment in a dose-dependent manner, with the difference being statistically significant compared with that in the control group.

CUDC-101 can regulate gene expression in T24 cells. RNA was extracted from the drug-treated cells, before transcriptome sequencing of the cells was completed using the Illumina sequencing platform (Figs. 1 and S1; Tables SI-IV), RNA was extracted from the drug-treated cells, before transcriptome sequencing of the cells was completed using the Illumina sequencing platform (Figs. 1 and S1; Tables SI-IV). After the drug treatment of T24 cells, the expression of 2,205 genes were found to be upregulated, including cytochrome P450 family 1 subfamily A member 1 (CYP1A1), transmembrane protein 59-like (TMEM59L) and TGFβ-induced (TGFBI). By contrast, the expression of 1,674 genes were found to be decreased, including erythroferrone (ERFE), UNC-5 netrin receptor B (UNC5B) and microRNA-503 host gene (MIR503HG). In T24-EGFR-OE cells, the expression of 2,651 genes [including retbindin (RTBDN), CYP1A1, TMEM59L and TGFBI] were found to be upregulated, whereas 1,988 genes [such as pappalysin 2, IL-1 receptor-like 1, ERFE, spectrin repeat containing nuclear envelope family member 3 (SYNE3) and thrombomodulin (THBD)] were found to be downregulated. As shown in Tables SI-IV, a number of genes with similar functions or with close associations with each other had their expression levels altered before and after drug administration in both groups of cells. All differentially expressed genes were then analyzed by GO and KEGG enrichment, where the top 30 most significantly enriched GO terms were selected (Figs. S2 and S3). In addition, the most significantly enriched pathway entries are shown in Figs. S4 and S5. The concentration and quality of the RNA samples are shown in Tables SV and SVI. The Pearson's correlation coefficients of the RNA samples are shown in Fig. S6.

CUDC-101 decreased the proliferative capacity of T24-EGFR-OE cells. GO enrichment analysis of genes that

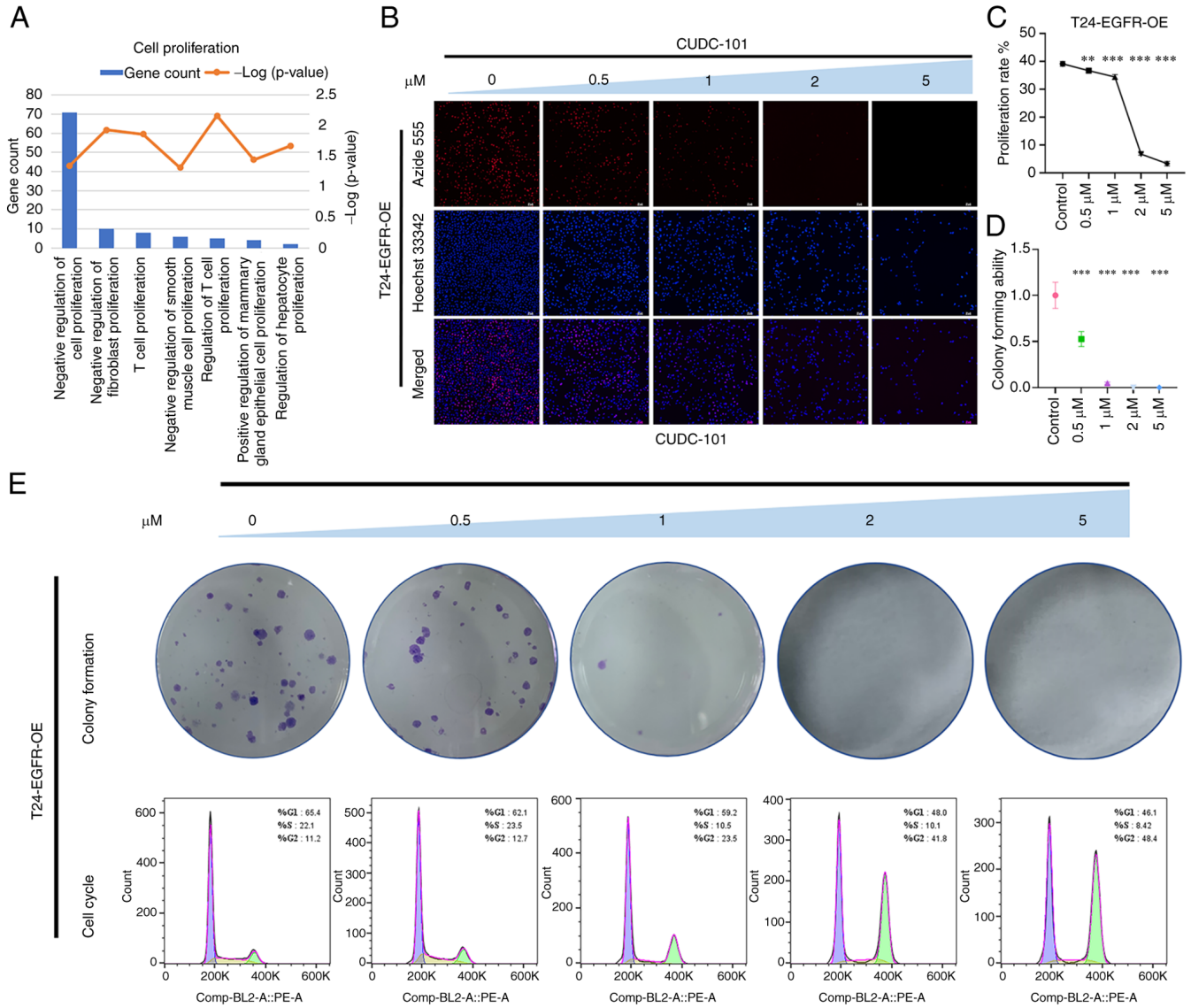

Figure 2. Effect of CUDC-101 on the proliferative capacity of T24-EGFR-OE cells. (A) The results of Gene Ontology enrichment analysis of the differentially expressed genes after CUDC-101 treatment on T24-EGFR-OE cells. (B) The results of EdU staining, Azide 555 was used to label the proliferative cells and Hoechst 33342 was used to label all nuclei. Magnification, x100; Scale bar, 50 μm. (C) Effects of CUDC-101 on the growth rates of T24-EGFR-OE cells at 0, 0.5, 1, 2 and 5 μM. The proliferation rate was obtained from the results of EdU experiment, where the concentrations were presented from high to low. Data are presented as mean ± SEM from three independent experiments. (D and E) The colony formation assay. Comparing the CUDC-101 groups with the control group, the percentage of the clone number in each group was calculated by normalizing to the control group, with the latter identified as '1'. Data are presented as the mean ± SEM from three independent experiments. **P<0.01 and ***P<0.001 vs. control. In the lower part of Fig. 2E are the cell cycle results. OE, overexpression.

were significantly differentially expressed in T24-EGFR-OE cells following CUDC-101 treatment revealed that the effects mediated by CUDC-101 was significantly associated with cell proliferation biological processes (Fig. 2A). As shown in Fig. 2B, the overall proportion of surviving cells after drug treatment was decreased compared with that in the control group, where number of proliferative cells 1 h after treatment was also decreased compared with that in the control group. Furthermore, the total number of cells and the number of proliferative cells decreased in magnitude as the drug concentration increased. The number of proliferating cells compared with the overall number of cells was used as the metric to calculate the proliferation rate of cells (Fig. 2C). The proliferation rate of the cells in the drug-treated groups was found to be lower compared with that in the control group, in a concentration-dependent manner.

As shown in Fig. 2E, the number of colonies in the experimental group was found to be lower compared with that in the control group after treatment with CUDC-101, also in a concentration-dependent manner. The number of colonies in the control group was set to 1, before the clonogenic capacity of cells in the drug-treated groups was obtained by dividing the number of colonies drugs-treated groups by that in the control group. As the concentration increased, the clonogenic capacity of the cells correspondingly decreased, with the difference between the CUDC-101-treated groups and the control group being significant (Fig. 2D). In particular, the 2 μM CUDC-101 group did not show any colony formation. The cell cycle assay results are shown in Fig. 2E. CUDC-101 treatment was found to decrease the number of cells in G_1- and S-phases whilst inducing G_2/M-phase cell aggregation in a dose-dependent

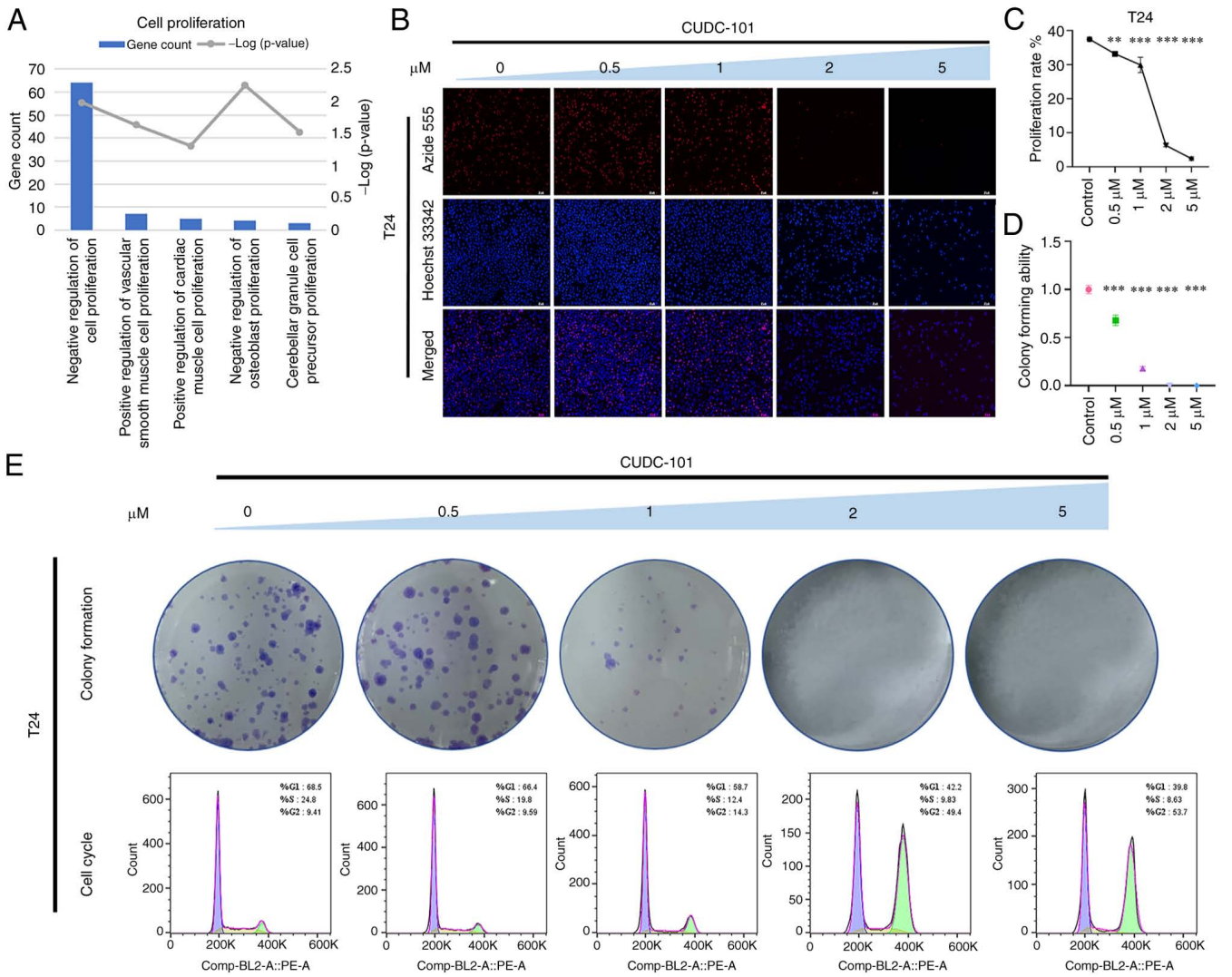

Figure 3. Effect of CUDC-101 on the proliferative capacity of T24 cells. (A) The results of Gene Ontology enrichment analysis of differentially expressed genes after CUDC-101 action on T24 cells. (B) Results of EdU staining. Azide 555 was used to label the proliferative cells and Hoechst 33342 was used to label all nuclei. Magnification, x100. Scale bar, 50 μm. (C) Effects of CUDC-101 treatment on the growth rates of T24 cells at 0, 0.5, 1, 2 and 5 μM. The proliferation rate was obtained from the results of EdU assay, where the concentrations were presented from high to low. Data are presented as the mean ± SEM from three independent experiments. (D and E) Colony formation assay results. Comparing the CUDC-101 groups to the control group, the percentage of the clone number in each group was calculated by normalizing to the control group, with the latter identified as '1'. Data are presented as the mean ± SEM from three independent experiments. **P<0.01 and ***P<0.001 vs. control. In the lower part of Fig. 3E are the cell cycle results.

manner. This suggested that CUDC-101 may have caused cell cycle arrest, which may be one of the causes of the inhibited cell proliferation.

CUDC-101 reduces the proliferative capacity of T24 cells. In T24 cells, the effects mediated by CUDC-101 was found to be significantly associated with cell proliferation or growth biological processes (Fig. 3A). The effect of CUDC-101 on the proliferation of T24 cells was also examined. As shown in Fig. 3B and C, the number of proliferative cells and the proliferation rate of cells showed a concentration-dependent decrease with increasing drug concentration. As shown in Fig. 3E, cell cycle was similarly blocked at the G_2/M phase, which may have caused the inhibition of cell proliferation. In addition, the number of T24 cell colonies was also found to be decreased compared with that in the control group after treatment with CUDC-101, which increased in magnitude decreased as the concentration of CUDC-101 increased (Fig. 3E). The colony-forming ability of the cells in the treated group was significantly lower compared with that in the control group (Fig. 3D). At 2 μM, the T24 cells were not able to form any colonies.

CUDC-101 promotes the apoptosis of T24-EGFR-OE cells. GO enrichment analysis of genes that were significantly differentially expressed in T24-EGFR-OE cells following CUDC-101 treatment showed that the effects mediated by CUDC-101 were significantly associated with apoptosis or death biological processes (Fig. 4A).

As shown in Fig. 4F, the cells in the control group exhibited normal cell shape. Furthermore, their microfilaments appear normal and evenly distributed with intact nuclei, where some cells also showed a number of microfilament tentacles. Following CUDC-101 treatment, the cell numbers decreased, with cells becoming aggregated and adherent. A number of cells also became irregular morphologically. In

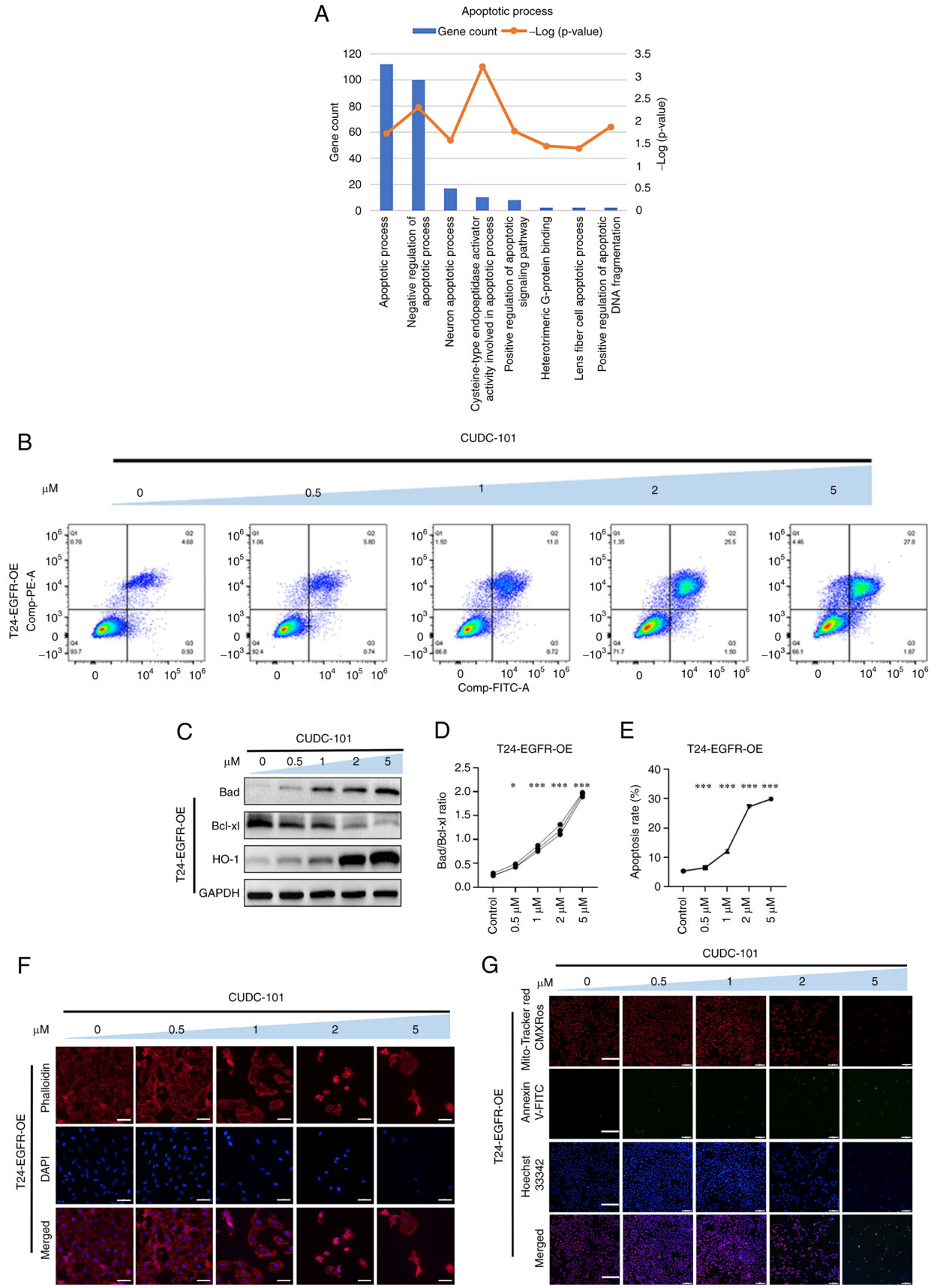

Figure 4. CUDC-101 promotes the apoptosis of T24-EGFR-OE cells. (A) Results of Gene Ontology enrichment analysis of differentially expressed genes after CUDC-101 treatment on T24-EGFR-OE cells. (B) The apoptosis levels of T24-EGFR-OE cells were detected by flow cytometry. (C) Expression of apoptotic marker proteins. (D) Semi-quantification of the Bad/Bcl-xl ratio in T24-EGFR-OE cells. (E) Semi-quantification of the apoptosis rate of T24-EGFR-OE cells in Q2 and Q3 after CUDC-101 treatment in (B). Data are presented as the mean ± SEM from three independent experiments. *P<0.05 and ***P<0.001 vs. control. (F) Changes in the nuclear and cytoskeletal microfibrils. Red represents the cytoskeleton whereas the blue represents the nucleus. Scale bar, 50 μm. (G) Mitochondrial membrane potential and apoptosis were detected by fluorescence microscopy. Red represents the mitochondrial membrane potential; blue is the nucleus; and green represents apoptotic cells. Scale bar, 150 μm. OE, overexpression.

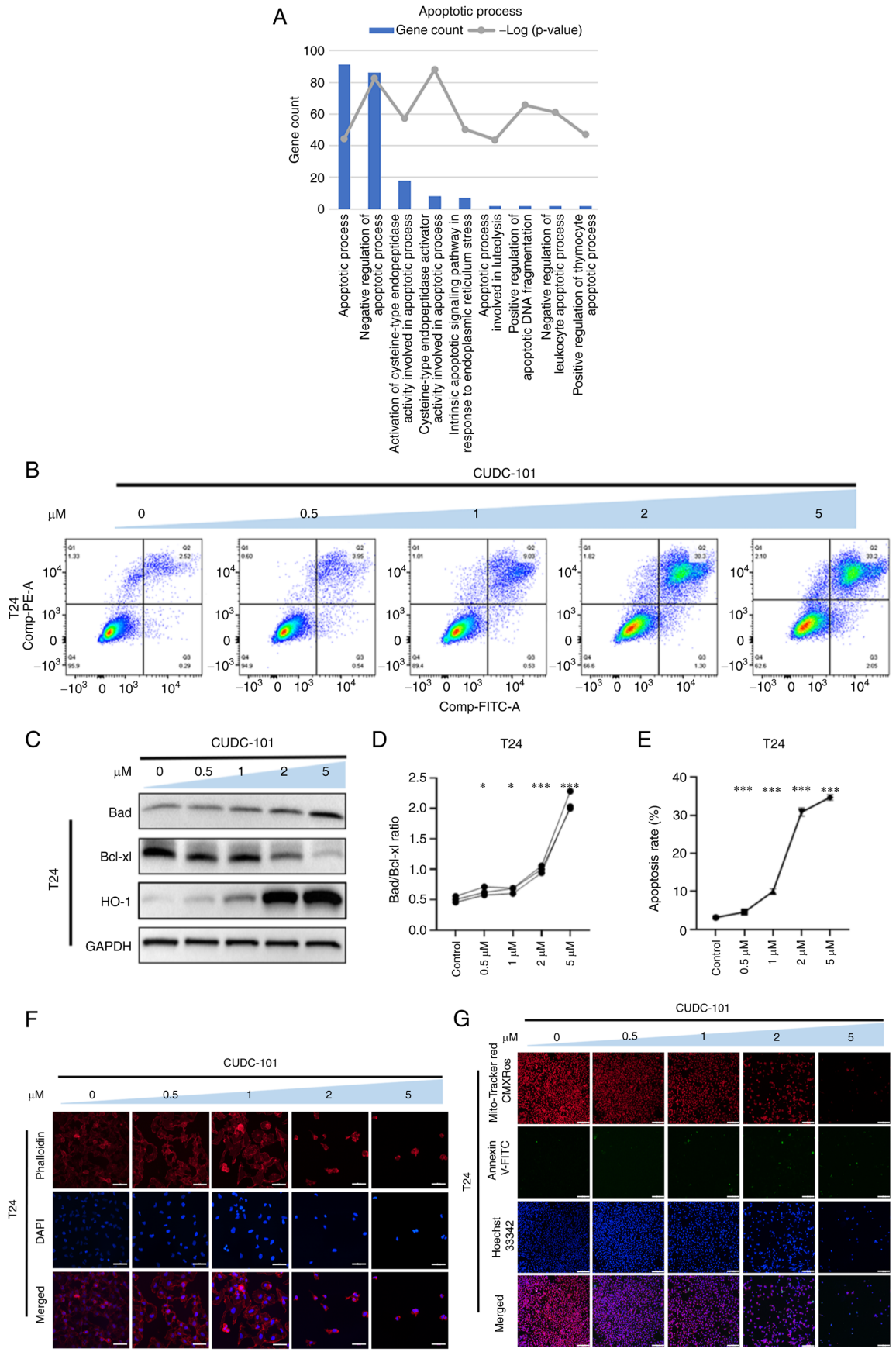

Figure 5. CUDC-101 promotes apoptosis in T24 cells. (A) Results of Gene Ontology enrichment analysis of differentially expressed genes after CUDC-101 treatment in T24 cells. (B) The apoptosis level of T24 cells was detected by flow cytometry. (C) Expression of apoptotic marker proteins. (D) Semi-quantification of the Bad/Bcl-xl ratio in T24 cells. (E) Semi-quantification of the apoptosis rate of T24 cells in Q2 and Q3 after CUDC-101 treatment in (B). Data are presented as the mean ± SEM from three independent experiments. *P<0.05 and ***P<0.001 vs. control. (F) Changes in the nucleus and cytoskeletal microfibrils. Red, cytoskeleton; bule, cell nucleus. Scale bar, 50 μm. (G) Mitochondrial membrane potential and apoptosis were detected by fluorescence. Red represents the mitochondrial membrane potential; blue is the nucleus; and green represents apoptotic cells. Scale bar, 150 μm.

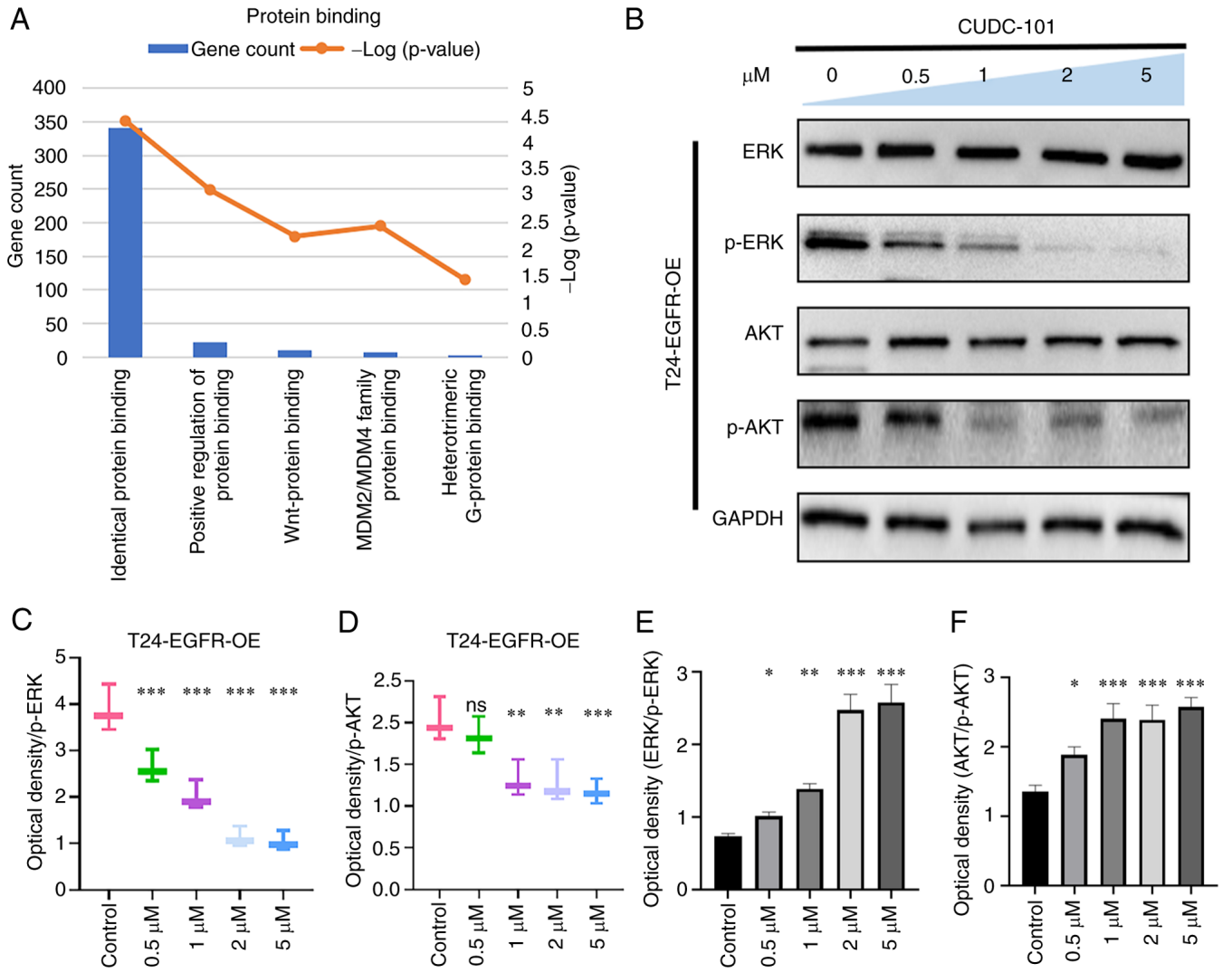

Figure 6. Effect of CUDC-101 on protein expression in T24-EGFR-OE cells. (A) Results of Gene Ontology enrichment analysis of differentially expressed genes after CUDC-101 action on T24-EGFR-OE cells. (B) Expression of ERK and AKT proteins. Measurement of (C) phosphorylated ERK, (D) AKT phosphorylation and (E) Total ERK/p-ERK ratio and (F) total AKT/p-AKT ratio following CUDC-101 treatment at 0.5-5 μM. *P<0.05, **P<0.01 and ***P<0.001 vs. control. OE, overexpression; p-, phosphorylated; ns, not significant.

addition, various cells ruptured with their microfilaments either maldistributed or wrinkled, with disrupted nuclei. These observations were found to be increase as dose of CUDC-101 increased. These results suggested that CUDC-101 can reduce the number of T24-EGFR-OE cells, alter the cell morphology and redistribute the cytoskeletal microfilament structure in the cells, in addition to inducing nucleus fragmentation or even cell death.

As shown in Fig. 4G, the overall number of cells was decreased after drug treatment compared with that the control group. Specifically, the degree of red fluorescence was decreased, suggesting that the mitochondrial membrane potential decreased after drug administration. Furthermore, the number of cells with green fluorescence was increased, suggesting that apoptosis was increased and that CUDC-101 exerted pro-apoptotic effects on T24-EGFR-OE cells. CUDC-101 also appeared to have reduced the mitochondrial membrane potential of T24 cells.

Apoptosis was next detected by Annexin V-FITC/PI fluorescent double-staining, and results showed that the percentage of apoptotic cells increased after drug treatment compared with the control group. This increase in apoptosis was also found to be dependent on the drug concentration (Fig. 4B and E).

As shown in Fig. 4C, the expression of the anti-apoptotic protein Bcl-xl decreased whereas that of Bad increased after drug treatment. The ratio of Bad/Bcl-xl was then obtained by calculation, where the difference was observed to be statistically significant between the drug-treated groups and the control group, suggesting that the apoptosis ratio was increased as the CUDC-101 concentration increased (Fig. 4D). The expression of the oxidative stress protein HO-1 was also increased in a concentration-dependent manner (Fig. 4C). These results suggested that CUDC-101 treatment promoted apoptosis in a concentration-dependent manner in T24-EGFR-OE cells.

CUDC-101 promotes the apoptosis of T24 cells. In T24 cells, the effects of CUDC-101 were significantly associated with apoptosis or death biological processes (Fig. 5A). As shown in Fig. 5F, T24 cells treated with CUDC-101 also changed in a similar manner to T24-EGFR-OE cells, in that a decreases in

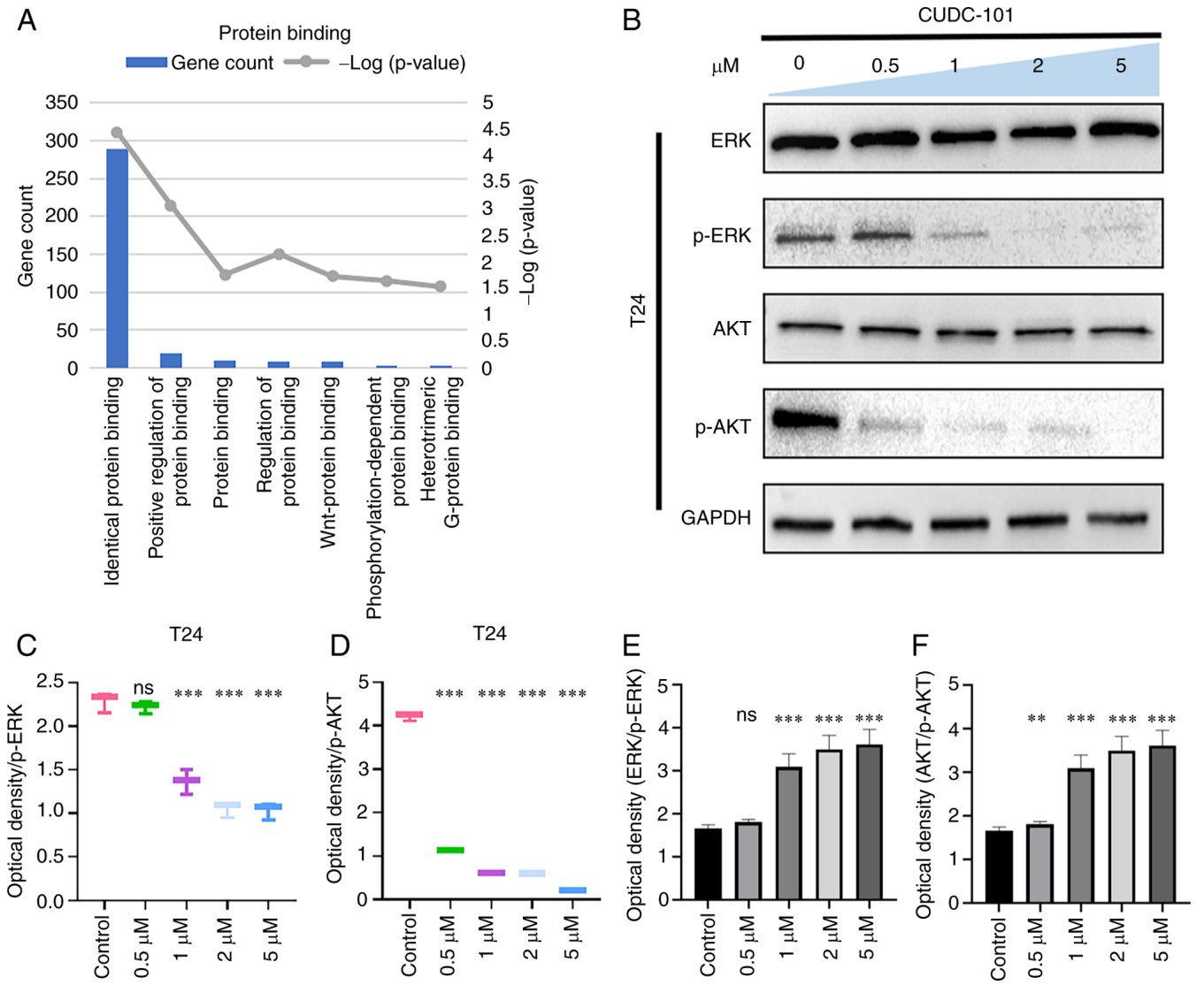

Figure 7. Effect of CUDC-101 on related protein expression in T24 cells. (A) Results of Gene Ontology enrichment analysis of differentially expressed genes after CUDC-101 action on T24 cells. (B) Expression of ERK and AKT proteins. Measurement of (C) phosphorylated ERK, (D) AKT phosphorylation and (E) Total ERK/p-ERK ratio and (F) total AKT/p-AKT ratio following CUDC-101 treatment at 0.5-5 μM. **P<0.01 and ***P<0.001 vs. control OE, overexpression; p-, phosphorylated; ns, not significant.

cell viability, cell aggregation and adhesion, some cells became exhibiting irregular morphology, cell rupture, poor microfilament distribution, wrinkled peripheral microfilaments and disrupted nuclei were all observed following CUDC-101 treatment. In addition, as the concentration of CUDC-101 increased, the aforementioned observations correspondingly worsened.

As shown in Fig. 5G, the total number of T24 cells was decreased and the number of apoptotic cells showing green fluorescence increased, whereas the mitochondrial membrane potential decreased, following drug administration, compared with those in the control group. As the concentration of CUDC-101 increased, the ratio of Bad/Bcl-xl also increased significantly compared with that in the control group. Expression of the oxidative stress protein HO-1 was also increased by CUDC-101 in a concentration-dependent manner (Fig. 5C). As shown in Fig. 5B, the number of Annexin V-FITC-positive cells was increased, suggesting that CUDC-101 can mediate similar pro-apoptotic effects on T24 cells.

Effects of CUDC-101 on AKT and ERK phosphorylation. As shown in Fig. S7, compared with those in T24 cells, the expression of EGFR and phosphorylation of EGFR were increased in the EGFR-overexpressing T24 cell line, both groups were cultured with 1640 medium and no special treatment, suggesting that the T24-EGFR-OE cell line was successfully constructed. As shown in Figs. 6 and 7, the expression of ERK and AKT did not change in T24 or T24-EGFR-OE cells, whilst the expression of phosphorylation of ERK and AKT decreased in response to CUDC-101 treatment in a concentration-dependent manner. This suggested that CUDC-101 can inhibit cell proliferation by promoting apoptosis through a number of signaling pathways.

Discussion

Bladder cancer is the most common malignancy in the genitourinary system, with high rates of morbidity and mortality (19). The majority of cases have poor prognosis with complex

etiology (20). Although advanced diagnostic techniques and surgical treatment have greatly improved the prognosis of bladder cancer (21,22), the treatment strategy for bladder cancers with certain genetic and expression mutation profiles remain less clear. Therefore, precise molecular targeting is not possible on certain bladder cancer cases where surgical treatment is also not possible (23).

In a previous study, bladder cancer with EGFR overexpression was found to be susceptible to targeted TKI afatinib, which can affect the proliferation and apoptosis of bladder cancer cells (24). However, the role of other targeted drugs on bladder cancer remain to be elucidated. Therefore, the present study explored a novel molecularly targeted therapeutic agent to enrich the number molecular treatment options for bladder cancer.

In the present study, the bladder cancer cell lines T24 was chosen as the model; this contain mutations in the RAS gene, the most common mutation among bladder cancer mutation types (25) and there is a large variation in positive EGFR expression in bladder cancer (26), which in T24 cells is shown in Fig. S7. A wild-type EGFR gene fragment was introduced into this cell line using the viral packaging method described previously (27) to create a bladder cancer cell model with EGFR overexpression for simulating patients with this type of bladder cancer. Subsequently, CUDC-101, a multi-targeted inhibitor of HDAC, EGFR and HER2 (28), was applied. CUDC-101 has been previously shown to inhibit cell proliferation in head and neck cancer (29), thyroid cancer (30) and pancreatic cancer (31), in addition to serving a role in reversing drug resistance and preventing cancer cell migration (32).

In the present study, MTT assay was used to detect the effects of CUDC-101 on cell survival and viability. It was found that CUDC-101 could inhibit cell proliferation in a dose- and time-dependent manner. EdU and colony assays were used to detect the effects of CUDC-101 on cell proliferation and it was found that it could inhibit cell proliferation in both T24 and T24-EGFR-OE cells in a dose-dependent manner. Flow cytometry was then used to detect the extent of apoptosis, which found that the degree of apoptosis was increased by CUDC-101 in a dose-dependent manner. These results suggested that CUDC-101 reduced cell viability and vigor while promoting apoptosis.

The present study additionally detected changes in cell morphology and internal structure. The cytoskeleton is the main mechanical structure within cells, which is formed by a complex network of dynamic biopolymers, such as microtubules, actin and intermediate filaments (33). In response to stimulation, cytoskeletal reorganization, microfilament bundle breakage and shrinkage will occur, ultimately leading to apoptotic cell death (34,35). The present study found that the cell membrane was uneven, where the nuclei appeared crinkled and fragmented following CUDC-101 treatment. In addition, the actin microfilament structure changed following drug treatment, suggesting that CUDC-101 could alter the distribution of cytoskeletal structures in both the T24 and T24-EGFR-OE cell lines, in turn promoting apoptosis (36). A normal transmembrane mitochondrial potential is necessary for maintaining mitochondrial function (37). Significant decreases in the mitochondrial transmembrane potential will irreversibly initiate the apoptotic process (38). In the present study, CUDC-101 was found to promote apoptosis in both cell lines. Flow cytometry results confirmed that CUDC-101 was able to significantly promote apoptosis in T24 and T24-EGFR-OE cells in a dose-dependent manner. These results suggested that CUDC-101 acted on bladder cancer cells by decreasing cell survival and viability, altering cytoskeletal structure, decreasing mitochondrial membrane potential, and ultimately promoting apoptosis.

Performed signaling pathways modulate the equilibrium between cell viability and apoptosis. In CUDC-101-treated bladder cancer cells, the effect of CUDC-101 on apoptosis via AKT and ERK signaling pathways was evaluated. The EGFR signaling pathway induces the mobilization of a number of pathways downstream, including PI3K, AKT, MAPK/ERK, protein kinase C (PKC), and JAK/STAT pathways (39). The results of the present study also suggested that in CUDC-101-treated bladder cancer cells, CUDC-101 could inhibit differentiation and enhanced apoptotic cell death through the PI3K/AKT and ERK cascade pathways. The PI3K/Akt and ERK signaling pathways are closely associated with tumor cell survival, invasion and metastasis (40) and PI3K/AKT inhibitors have been explored as therapeutic agents for tumor treatment (41). The results of the present study showed effects on the inactivation of PI3K/AKT and ERK pathways, thus demonstrating the potential ability of CUDC-101 to be used as a PI3K/AKT inhibitor for the treatment of bladder cancer.

However, the mechanisms of the CUDC-101-mediated pathway remain to be elucidated. In the present study, RNA-sequencing was used for further exploration and supplementary material provided the expression profiles of differentiated expressed genes in CUDC-101-treated cells. Transcriptome sequencing showed similar changes on the expression profiles in T24 and T24-EGFR-OE, suggesting that the regulation genes by CUDC-101 could be responsible for affecting cell growth, inhibiting cell proliferation. The next step in our research program is to refine the validation of the effects of CUDC-101 on the expression of these genes and data using a variety of cell lines, and to perform animal studies to eliminate the current limitations of this study due to the lack of *in vivo* experiments.

In conclusion, results from the present study suggest that CUDC-101 can reduce cell viability, inhibit cell proliferation, alter cell morphology and promote cell apoptosis on both T24 cells and T24 EGFR-overexpressed cells. These findings support a novel strategy for using CUDC-101 as a targeted inhibitor for EGFR-overexpressing bladder cancer clinical treatment.

Acknowledgements

Not applicable.

Funding

The present study was supported by the Teaching reform research and practice project of Henan University (grant no. 146) and the Research Project of Institutes of Traditional Chinese Medicine of Henan University (grant no. 2021YJYJZ06).

Availability of data and materials

The SRA records will be accessible with the following link after the indicated release date: https://www.ncbi.nlm.nih.gov/sra/PRJNA1010990. Accession to cite for these SRA data: PRJNA1010990. Temporary Submission ID: SUB13808738.

Authors' contributions

LA, XL and YW conceived and designed the study. ZW, LL and CC performed the experiments. XW, QL, RW, GZ and GW analyzed the data. LA and XL wrote the manuscript. ZW, LL and CC confirm the authenticity of all the raw data. All authors read and approved the final manuscript.

Ethics approval and consent to participate

Not applicable.

Patient consent for publication

Not applicable.

Completing interests

The authors declare that they have no competing interests.

References

1. Dobruch J and Oszczudlowski M: Bladder cancer: Current challenges and future directions. Medicina (Kaunas) 57: 749, 2021.
2. Sung H, Ferlay J, Siegel RL, Laversanne M, Soerjomataram I, Jemal A and Bray F: Global cancer statistics 2020: GLOBOCAN estimates of incidence and mortality worldwide for 36 cancers in 185 countries. CA Cancer J Clin 71: 209-249, 2021.
3. Kim IH and Lee HJ: Perioperative systemic treatment for muscle-invasive bladder cancer: Current evidence and future perspectives. Int J Mol Sci 22: 7201, 2021.
4. Lenis AT, Lec PM, Chamie K and Mshs MD: Bladder cancer: A review. JAMA 324: 1980-1991, 2020.
5. Guo CC and Czerniak B: Bladder cancer in the genomic era. Arch Pathol Lab Med 143: 695-704, 2019.
6. Masuda H, Zhang D, Bartholomeusz C, Doihara H, Hortobagyi GN and Ueno NT: Role of epidermal growth factor receptor in breast cancer. Breast Cancer Res Treat 136: 331-345, 2012.
7. O'Leary C, Gasper H, Sahin KB, Tang M, Kulasinghe A, Adams MN, Richard DJ and O'Byrne KJ: Epidermal growth factor receptor (EGFR)-mutated non-small-cell lung cancer (NSCLC). Pharmaceuticals (Basel) 13: 273, 2020.
8. Jaiswal BS, Kljavin NM, Stawiski EW, Chan E, Parikh C, Durinck S, Chaudhuri S, Pujara K, Guillory J, Edgar KA, *et al*: Oncogenic ERBB3 mutations in human cancers. Cancer Cell 23: 603-617, 2013.
9. Roskoski R Jr: The ErbB/HER family of protein-tyrosine kinases and cancer. Pharmacol Res 79: 34-74, 2014.
10. Arteaga CL and Engelman JA: ERBB receptors: From oncogene discovery to basic science to mechanism-based cancer therapeutics. Cancer Cell 25: 282-303, 2014.
11. Sabbah DA, Hajjo R and Sweidan K: Review on epidermal growth factor receptor (EGFR) structure, signaling pathways, interactions, and recent updates of EGFR inhibitors. Curr Top Med Chem 20: 815-834, 2020.
12. Sigismund S, Avanzato D and Lanzetti L: Emerging functions of the EGFR in cancer. Mol Oncol 12: 3-20, 2018.
13. Wang Z: ErbB receptors and cancer. Methods Mol Biol 1652: 3-35, 2017.
14. Lai CJ, Bao R, Tao X, Wang J, Atoyan R, Qu H, Wang DG, Yin L, Samson M, Forrester J, *et al*: CUDC-101, a multitargeted inhibitor of histone deacetylase, epidermal growth factor receptor, and human epidermal growth factor receptor 2, exerts potent anticancer activity. Cancer Res 70: 3647-3656, 2010.
15. Wang J, Pursell NW, Samson ME, Atoyan R, Ma AW, Selmi A, Xu W, Cai X, Voi M, Savagner P and Lai CJ: Potential advantages of CUDC-101, a multitargeted HDAC, EGFR, and HER2 inhibitor, in treating drug resistance and preventing cancer cell migration and invasion. Mol Cancer Ther 12: 925-936, 2013.
16. Shimizu T, LoRusso PM, Papadopoulos KP, Patnaik A, Beeram M, Smith LS, Rasco DW, Mays TA, Chambers G, Ma A, *et al*: Phase I first-in-human study of CUDC-101, a multitargeted inhibitor of HDACs, EGFR, and HER2 in patients with advanced solid tumors. Clin Cancer Res 20: 5032-5040, 2014.
17. Cai X, Zhai HX, Wang J, Forrester J, Qu H, Yin L, Lai CJ, Bao R and Qian C: Discovery of 7-[4-(3-ethynylphenylamino)-7-methoxyquinazolin-6-yloxy]-N-hydroxyheptanamide (CUDc-101) as a potent multi-acting HDAC, EGFR, and HER2 inhibitor for the treatment of cancer. J Med Chem 53: 2000-2009, 2010.
18. Galloway TJ, Wirth LJ, Colevas AD, Gilbert J, Bauman JE, Saba NF, Raben D, Mehra R, Ma AW, Atoyan R, *et al*: A Phase I study of CUDC-101, a multitarget inhibitor of HDACs, EGFR, and HER2, in combination with chemoradiation in patients with head and neck squamous cell carcinoma. Clin Cancer Res 21: 1566-1573, 2015.
19. Martinez Rodriguez RH, Buisan Rueda O and Ibarz L: Bladder cancer: Present and future. Med Clin (Barc) 149: 449-455, 2017 (In English, Spanish).
20. Dobruch J, Daneshmand S, Fisch M, Lotan Y, Noon AP, Resnick MJ, Shariat SF, Zlotta AR and Boorjian SA: Gender and bladder cancer: A collaborative review of etiology, biology, and outcomes. Eur Urol 69: 300-310, 2016.
21. Pham A and Ballas LK: Trimodality therapy for bladder cancer: Modern management and future directions. Curr Opin Urol 29: 210-215, 2019.
22. Ahmadi H, Duddalwar V and Daneshmand S: Diagnosis and staging of bladder cancer. Hematol Oncol Clin North Am 35: 531-541, 2021.
23. Seidl C: Targets for therapy of bladder cancer. Semin Nucl Med 50: 162-170, 2020.
24. Tang Y, Zhang X, Qi F, Chen M, Li Y, Liu L, He W, Li Z and Zu X: Afatinib inhibits proliferation and invasion and promotes apoptosis of the T24 bladder cancer cell line. Exp Ther Med 9: 1851-1856, 2015.
25. Przybojewska B, Jagiello A and Jalmuzna P: H-RAS, K-RAS, and N-RAS gene activation in human bladder cancers. Cancer Genet Cytogenet 121: 73-77, 2000.
26. Denny WA: The 4-anilinoquinazoline class of inhibitors of the erbB family of receptor tyrosine kinases. Farmaco 56: 51-56, 2001.
27. An L, Wang Y, Wu G, Wang Z, Shi Z, Liu C, Wang C, Yi M, Niu C, Duan S, *et al*: Defining the sensitivity landscape of EGFR variants to tyrosine kinase inhibitors. Transl Res 255: 14-25, 2023.
28. Sun H, Mediwala SN, Szafran AT, Mancini MA and Marcelli M: CUDC-101, a novel inhibitor of full-length androgen receptor (flAR) and androgen receptor variant 7 (AR-V7) activity: Mechanism of action and in vivo efficacy. Horm Cancer 7: 196-210, 2016.
29. Oliveira-Silva RJ, Carolina de Carvalho A, de Souza Viana L, Carvalho AL and Reis RM: Anti-EGFR therapy: Strategies in head and neck squamous cell carcinoma. Recent Pat Anticancer Drug Discov 11: 170-183, 2016.
30. Zhang L, Zhang Y, Mehta A, Boufraqech M, Davis S, Wang J, Tian Z, Yu Z, Boxer MB, Kiefer JA, *et al*: Dual inhibition of HDAC and EGFR signaling with CUDC-101 induces potent suppression of tumor growth and metastasis in anaplastic thyroid cancer. Oncotarget 6: 9073-9085, 2015.
31. Moertl S, Payer S, Kell R, Winkler K, Anastasov N and Atkinson MJ: Comparison of radiosensitization by HDAC inhibitors CUDC-101 and SAHA in pancreatic cancer cells. Int J Mol Sci 20: 3529, 2019.
32. Bass AKA, El-Zoghbi MS, Nageeb EM, Mohamed MFA, Badr M and Abuo-Rahma GEA: Comprehensive review for anticancer hybridized multitargeting HDAC inhibitors. Eur J Med Chem 209: 112904, 2021.
33. Pegoraro AF, Janmey P and Weitz DA: Mechanical properties of the cytoskeleton and cells. Cold Spring Harb Perspect Biol 9: a022038, 2017.
34. Bottone MG, Santin G, Aredia F, Bernocchi G, Pellicciari C and Scovassi AI: Morphological features of organelles during apoptosis: An overview. Cells 2: 294-305, 2013.

35. Liu C, Wang Z, Liu Q, Wu G, Chu C, Li L, An L and Duan S: Sensitivity analysis of EGFR L861Q mutation to six tyrosine kinase inhibitors. Clin Transl Oncol 24: 1975-1985, 2022.
36. Annesley SJ and Fisher PR: Mitochondria in health and disease. Cells 8: 680, 2019.
37. Sakamuru S, Attene-Ramos MS and Xia M: Mitochondrial membrane potential assay. Methods Mol Biol 1473: 17-22, 2016.
38. Hussain S: Measurement of nanoparticle-induced mitochondrial membrane potential alterations. Methods Mol Biol 1894: 123-131, 2019.
39. Chong CR and Jänne PA: The quest to overcome resistance to EGFR-targeted therapies in cancer. Nat Med 19: 1389-1400, 2013.
40. Yue X, Li M, Chen D, Xu Z and Sun S: UNBS5162 induces growth inhibition and apoptosis via inhibiting PI3K/AKT/mTOR pathway in triple negative breast cancer MDA-MB-231 cells. Exp Ther Med 16: 3921-3928, 2018.
41. Yang Q, Modi P, Newcomb T, Quéva C and Gandhi V: Idelalisib: First-in-class PI3K delta inhibitor for the treatment of chronic lymphocytic leukemia, small lymphocytic leukemia, and follicular lymphoma. Clin Cancer Res 21: 1537-1542, 2015.